

PHYSICAL REVIEW B

CONDENSED MATTER

THIRD SERIES, VOLUME 43, NUMBER 8

15 MARCH 1991-I

Charge-density-wave dynamics in $(\text{Ta}_{1-x}\text{Nb}_x\text{Se}_4)_2\text{I}$ alloys

Tae Wan Kim, S. Donovan, and G. Grüner

Department of Physics and Solid State Science Center, University of California, Los Angeles, Los Angeles, California 90024

A. Philipp

Institut für Festkörperphysik der Universität Wien and Ludwig Boltzmann Institut für Festkörperphysik, Kopernikusgasse 15, A-1050 Wien, Austria

(Received 18 June 1990)

Frequency-dependent conductivity and phase-resolved harmonic-mixing studies are reported on alloys of the linear-chain compound $(\text{TaSe}_4)_2\text{I}$ with Nb in the microwave and millimeter-wave spectral range. The frequency-dependent conductivity is evaluated in the charge-density-wave (CDW) state, and the collective-mode response is analyzed in terms of a harmonic-oscillator response with an effective mass m^* , a pinning frequency ω_0 , and relaxation time τ^* as parameters. We find that the magnitude, temperature, and concentration dependence of the effective mass m^* is well described in terms of the mean-field description of the dynamical CDW response. The pinning frequency ω_0 increases with increasing impurity concentration x , and the concentration dependence is suggestive of strong-impurity pinning. We also evaluate the temperature and concentration dependence of the relaxation time τ^* , and compare this parameter with various models.

I. INTRODUCTION

Impurities have a profound influence on both the static and dynamic properties of the Peierls-Fröhlich charge-density-wave (CDW) state.¹ The impurity potential couples directly to the phase ϕ of the condensate and this leads to the absence of long-range order in less than four dimensions.² One important consequence of this is the smearing of the phase transition, as evidenced by various experiments on different model compounds. Impurities also lead to pinning of the phase and to the elastic deformation of the collective mode around impurities, and the impurity-CDW interaction shifts the oscillator strength to finite frequencies.

In spite of a considerable amount of experimental and theoretical work, relatively little is known about the fundamental parameters which determine the dynamics of charge-density waves.³⁻⁵ Our experiments on $\text{K}_{0.3}\text{MoO}_3$ and $(\text{TaSe}_4)_2\text{I}$ conducted in the microwave and millimeter-wave spectral range, when combined with the optical^{6,7} studies and experiments conducted at radio-frequencies,⁸ lead to a frequency-dependent conductivity which is displayed⁹ in Fig. 1. The inset shows the low-frequency part of the optical conductivity in detail. In Fig. 1 four distinct features are apparent. The rise of the

real part of the conductivity $\sigma = \text{Re}\sigma + i\text{Im}\sigma$, $\text{Re}\sigma$ in the infrared spectral range is due to single-particle excitations across the gap. The arrow denoted by ω_g represents the single-particle gap determined by the temperature dependence of the dc conductivity, which is given well below T_p by $\sigma = \sigma_0 \exp(-\Delta/k_B T)$. This leads to $\Delta \approx 1500 \text{ cm}^{-1}$ for $(\text{TaSe}_4)_2\text{I}$. In the radio-frequency spectral range, the (strongly temperature dependent) broad tail which is displayed in the inset of Fig. 1 is related to the internal deformations of the phason mode, and both quantum-mechanical¹⁰ and classical¹¹ descriptions of $\sigma(\omega)$ in this spectral range are available. In all of these models, the relevant frequency where the broad feature appears is given by $\omega_T(T) = 4\pi\sigma_{\text{dc}}(T)/\epsilon$, where ϵ is the dielectric constant associated with the high-frequency excitations and σ_{dc} is the dc conductivity which freezes out exponentially with decreasing temperatures. Numerical values of $\sigma_{\text{dc}}(T)$ and ϵ describe well the observed magnitude and temperature dependence of the radio-frequency resonance. The resonance at ω_0 , the so-called pinning frequency, occurs at 1 cm^{-1} for $(\text{TaSe}_4)_2\text{I}$ and it is due to the oscillatory response of the collective mode. The mode at approximately 20 cm^{-1} has not been clearly identified.⁹

In this paper we report on our experiments conducted

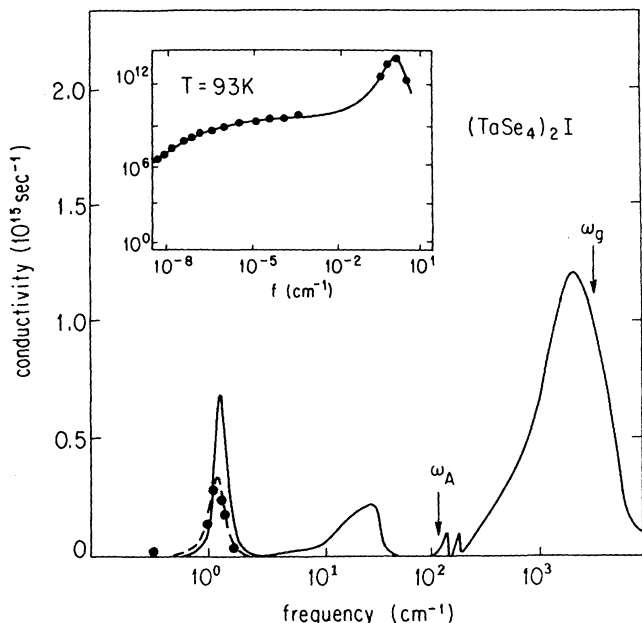


FIG. 1. Optical conductivity for $(\text{TaSe}_4)_2\text{I}$ as evaluated from the Kramers-Kronig analysis. The solid points are $\text{Re}\sigma(\omega)$ values evaluated directly from microwave and millimeter-wave experiments, and the dotted line is a fit to a harmonic-oscillator expression of this response. The arrows represent the single-particle gap ω_g , and the amplitude-mode frequency ω_A .

in the spectral range which includes the resonance associated with the pinned collective mode, which in the pure compound appears at frequencies close to 1 cm^{-1} .

While various experiments in a range of model compounds have been interpreted¹ by assuming that the response is that of a single-harmonic oscillator,

$$\frac{d^2x}{dt^2} + \frac{1}{\tau^*} \frac{dx}{dt} + \omega_0^2 x = \frac{eE}{m^*} e^{i\omega t}, \quad (1)$$

with an effective mass m^* , damping constant τ^* , and pinning frequency ω_0 ; little is known about the detailed temperature and impurity dependence of these quantities. The effective mass is significantly larger than the band mass, and reflects the response of the coupled electron-phonon system to external perturbations.¹ In general, the pinning frequency is found to be increasing with the impurity concentration,⁵ which is in agreement with currently accepted models of charge-density-wave dynamics. However, the various origins of the spectral width of the resonance are not clear at present.

While the frequency-dependent conductivity represents the small-amplitude response of the collective mode, pronounced nonlinear effects also occur both at dc and at higher frequencies. Combined ac-dc excitation experiments have been conducted mainly in the radio-frequency spectral range;¹² at microwave frequencies, the technique called phase-resolved harmonic mixing¹³ has been most useful to explore the nonlinear dynamics of pinned charge-density waves. In the past phase-resolved mi-

crowave harmonic mixing (PREHM) has been used for extensive studies of the nonlinear behavior of the conductivity in pure trichalcogenides like NbSe_3 (Refs. 13 and 14) and TaS_3 (Ref. 15) as well as in the tetrachalcogenide $(\text{TaSe}_4)_2\text{I}$.¹⁶ The mixing signal was measured as a function of temperature, of the amplitude of the microwaves, and of their frequency. The results were in qualitative agreement with the tunneling model¹⁷ while a calculation by Matsukawa¹⁸ based on the Fukuyama-Lee-Rice model¹⁹ leads only to a semiquantitative description of the experimental findings.¹⁶ The dependence of the dynamical parameters, m^* , ω_0 , and τ^* on the Nb concentration x in $(\text{Ta}_{1-x}\text{Nb}_x\text{Se}_4)_2\text{I}$ may offer a possibility to discriminate between the various theories.

In this paper we report the first detailed experiments on the effect of impurities on the fundamental parameters of the collective-mode response in $(\text{TaSe}_4)_2\text{I}$ and its alloys $(\text{Ta}_{1-x}\text{Nb}_x\text{Se}_4)_2\text{I}$. The experiments were performed in the microwave and millimeter-wave spectral range where the pinned-mode resonance occurs for the pure compound, and, as we will demonstrate also for the alloys. In contrast to other materials like NbSe_3 or TaS_3 partial gapping of the Fermi surface, or possible commensurability effects do not occur, and consequently both the temperature and impurity dependence of the CDW dynamics can be studied in a broad range of parameters. Previous frequency-dependent studies on TaS_3 (Ref. 5) clearly established the role played by impurities, but because of complications mentioned above the detailed concentration and temperature dependence of the fundamental parameters of the problem have not been established.

II. EXPERIMENTAL TECHNIQUES AND RESULTS

Pure $(\text{TaSe}_4)_2\text{I}$ and its alloys $(\text{Ta}_{1-x}\text{Nb}_x\text{Se}_4)_2\text{I}$ were prepared by standard temperature-gradient furnace techniques. Crystals with typical sizes of $1 \text{ mm} \times 1 \text{ mm} \times 1 \text{ cm}$ have been obtained with the long axis corresponding to the chain axis. In the crystals the chain direction can be easily identified, and all experiments reported here in this paper refer to the conductivity and dielectric constant measured in this direction. The Nb concentration of the alloys was determined by wet-chemical analysis. The Peierls transition temperatures T_p for the onset of the charge-density-wave state ($T_p = 263 \text{ K}$ for the purest specimens prepared by us) were also determined on several specimens from the same batch, and subsequently an $x(T_p)$ curve was constructed. All specimens were subsequently characterized by measuring their transition temperatures. We have found slight differences in T_p for nominally pure materials from different preparation batches, reflecting different residual impurity levels. The sensitivity of chemical analysis was, however, not sufficient to evaluate the residual impurity concentration.

The microwave and millimeter-wave response was measured by using either a cavity-perturbation technique or a waveguide-bridge configuration with multiple-frequency measurements in each waveguide band.²⁰ The real and imaginary parts of the conductivity, $\text{Re}\sigma(\omega)$ and $\text{Im}\sigma(\omega)$, were evaluated using standard analysis. The

conductivity is related to the dielectric constant through the relation $\text{Re}\epsilon(\omega) = 4\pi \text{Im}\sigma(\omega)/\omega$. While $\text{Re}\sigma(\omega)$ was in all cases within 30% of the dc value at room temperature, this value is representative of the uncertainty of the analysis. Consequently, we have normalized all of the conductivity data to the dc conductivity $\sigma_{dc} = 350 \Omega^{-1} \text{cm}^{-1}$ at room temperature, by assuming that $\text{Re}\sigma(\omega)$ depends only weakly on x in the metallic range for small impurity concentrations.

The phase-resolved harmonic-mixing (PREHM) method used for the detection of the nonlinear ac conductivity is described in detail elsewhere²¹ and in the following is therefore sketched only briefly. A microwave of frequency ω and amplitude E_ω is mixed in a sample with its second harmonic of amplitude $E_{2\omega}$. Thus the time dependence of the applied microwave field is given by $E(t) = E_\omega \cos(\omega t + \phi) + E_{2\omega} \cos(2\omega t)$, where ϕ is the phase difference between the two frequencies. The nonlinear part of the current-voltage characteristic of the sample gives rise to a dc-voltage V_{mix} at the ends of the sample which depends on the phase difference ϕ . This mixing signal V_{mix} is recorded as a function of ϕ , which is continuously varied by a motor-driven phase shifter. An on-line Fourier analysis yields the amplitude V_2 of the $\cos(2\phi)$ -dependent component of $V_{\text{mix}}(\phi)$. This component is the predominant one and is therefore used for a comparison between experiment and theory. The phase-resolved detection allows us to discriminate spurious side effects which do not depend on ϕ , such as, e.g., thermoelectric voltages at the sample ends.

In Fig. 2 we display the temperature dependence of the low-field dc resistivities of pure $(\text{TaSe}_4)_2\text{I}$ and its alloys $(\text{Ta}_{1-x}\text{Nb}_x\text{Se}_4)_2\text{I}$ measured by a conventional four-probe method. The phase transition of pure $(\text{TaSe}_4)_2\text{I}$ at 263 K is not evident from the figure, but the peak position in the temperature derivative of the dc resistivity,

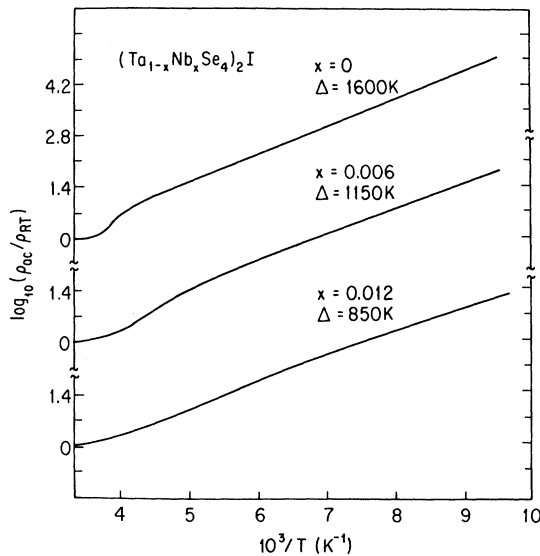


FIG. 2. Temperature dependence of the dc resistivity in $(\text{Ta}_{1-x}\text{Nb}_x\text{Se}_4)_2\text{I}$ alloys. The gap values evaluated from the temperature dependence of ρ_{dc} are given in the figure.

$d(\ln\rho_{dc})/d(1/T)$, signals the Peierls transition, as in other low-dimensional conductors.¹ The temperature derivative $d(\ln\rho_{dc})/d(1/T)$ of the dc resistivity shown in Fig. 3 clearly demonstrates the effect of impurities on the phase transition. We observe a progressive smearing of the transition, and also a gradual shift of the peak of the derivative to lower temperatures. Strictly speaking there is no phase transition to a CDW state with long-range order for an impure system, as mentioned earlier, however, as an operational definition we take the peak of $d(\ln\rho_{dc})/d(1/T)$ as the “transition temperature,” T_p .

The low-temperature value in Fig. 3 is related to the zero-temperature energy gap, as for a semiconductor with $\sigma = \sigma_0 \exp(-\Delta/k_B T)$, $d(\ln\rho)/d(1/T) = \Delta$. Consequently, from Fig. 3 the concentration dependence of Δ can also be established. We note, however, that due to the absence of long-range order, only a pseudogap is expected, leading also to deviations from the purely exponential temperature dependence of the dc conductivity. It is, however, apparent from Fig. 3 that this effect is small, and an average, or main gap Δ can firmly be established. In Fig. 4 we display T_p and Δ versus the Nb concentration. We observe a linear decrease in T_p and Δ with increasing impurity concentration, and the solid line corresponds to

$$\frac{dT_p}{dx} = -53 \text{ K/at. } \% , \quad (2a)$$

$$\frac{d\Delta}{dx} = -625 \text{ K/at. } \% . \quad (2b)$$

The linear depression of T_p is similar to that found in other linear-chain CDW compounds, such as TaS_3 and NbSe_3 .^{5,22} The concentration dependence of the gap has not been evaluated in earlier studies. For $(\text{TaSe}_4)_2\text{I}$ it may arise as a consequence of the change of band filling or size effects. We do not address this issue, but will use the observed concentration dependences in order to test

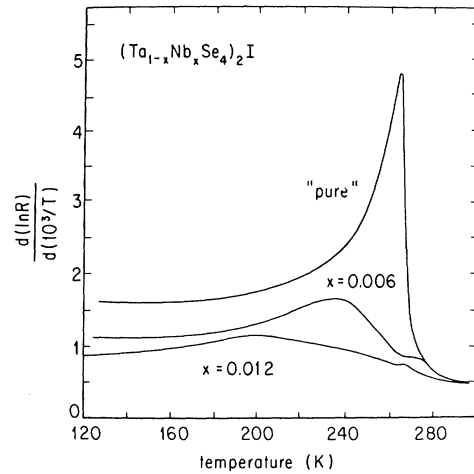


FIG. 3. Temperature dependence of the dc resistivity derivative $d(\ln\rho_{dc})/d(1/T)$ in $(\text{Ta}_{1-x}\text{Nb}_x\text{Se}_4)_2\text{I}$ alloys. Note that for a semiconductor, with $\sigma = \sigma_0 \exp(-\Delta/k_B T)$, the derivative corresponds to Δ for $T \ll T_p$.

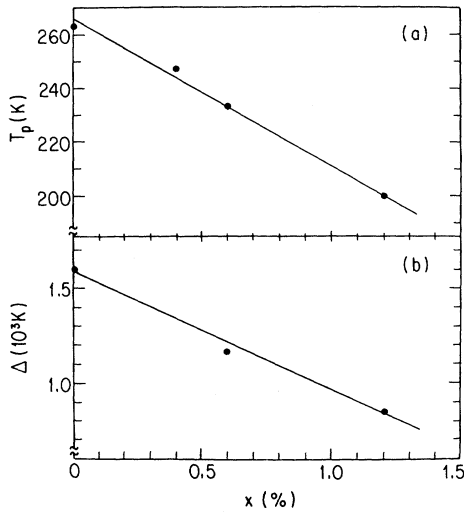


FIG. 4. Concentration dependence of the transition temperature, defined as the maximum in $d(\ln\rho_{dc})/d(1/T)$, and the low-temperature ($T \ll T_p$) gap in $(\text{Ta}_{1-x}\text{Nb}_x\text{Se}_4)_2\text{I}$ alloys.

various models of charge-density-wave dynamics. The reported value⁵ for TaS_3 is $dT_p/dx \approx -70$ K/at.%, a value similar to the one given by Eq. (2a). The conductivity $\text{Re}\sigma$ and dielectric constant $\text{Re}\epsilon$ measured at dc and also at various millimeter-wave frequencies are displayed in Fig. 5 for nominally pure $(\text{TaSe}_4)_2\text{I}$. A strongly frequency-dependent dispersion is found below Peierls transition temperature T_p in the millimeter-wave spectral range. The overall frequency dependence also suggests that a strong resonance occurs around approxi-

mately 30 GHz over the entire temperature range and the resonance becomes progressively sharper as the temperature is reduced. Also, the maximum conductivity $\sigma_{\text{max}}(\omega_0)$, which arises at ω_0 , the resonance frequency (which is located around 30 GHz), continues to increase as the temperature is lowered, much in the fashion which occurs for a metal.

The temperature dependence of the ac conductivity and dielectric constant is displayed in Fig. 6 for the alloy with $x=0.012$. A significant frequency dependence is again observed; however, the frequency where $\text{Re}\sigma$ has its maximum has shifted to higher frequencies, and for this specimen the maximum conductivity occurs at a frequency close to 130 GHz. The experimental results for the impurity concentration $x=0.006$ lie between those obtained for the "pure" and strongly doped specimens, displayed in Figs. 5 and 6 with a maximum conductivity occurring around $\omega_0/2\pi=60$ GHz.

The PREHM results on pure $(\text{TaSe}_4)_2\text{I}$ have been published in detail earlier¹⁶ and Fig. 7 shows the temperature dependence of V_2 at a fundamental frequency $\omega/2\pi=9.5$ GHz and at a temperature of 214 K. Also included in Fig. 7 are results obtained on two different $(\text{Ta}_{1-x}\text{Nb}_x\text{Se}_4)_2\text{I}$ alloys with values of $x=0.0045$ and 0.0065. The impurity concentration was determined from the Nb-concentration dependence of the Peierls temperature as given in Fig. 4. From Fig. 7 it follows that for $x=0.0045$ the mixing-signal component V_2 is by a factor of 3.5 larger than in the pure material and for $x=0.0065$ by even a factor of 7. The dependence of V_2 on the microwave amplitude E_ω for a constant ratio $E_\omega/E_{2\omega}$ corresponds to an E_ω^3 in the alloys, too, as has been earlier found in the pure materials.¹³⁻¹⁶

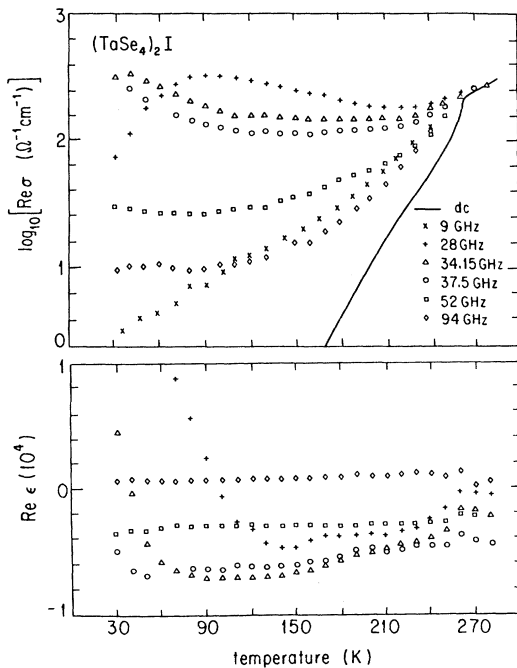


FIG. 5. Temperature dependence of $\text{Re}\sigma$ and $\text{Re}\epsilon$ of nominally pure $(\text{TaSe}_4)_2\text{I}$ at various frequencies.

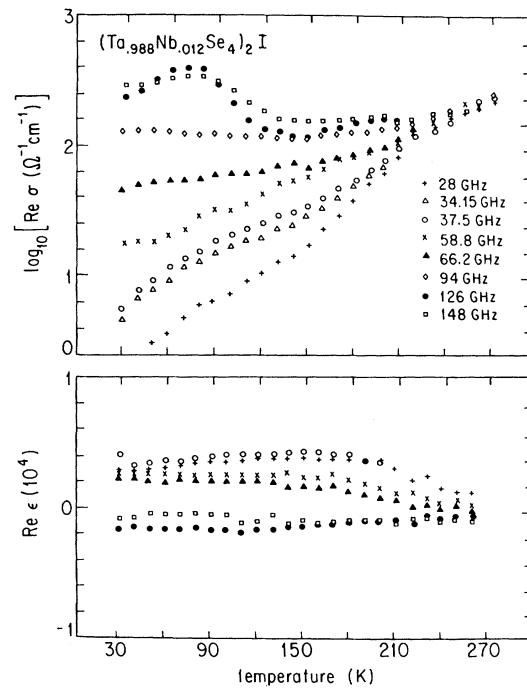


FIG. 6. Temperature dependence of $\text{Re}\sigma$ and $\text{Re}\epsilon$ of $(\text{Ta}_{0.988}\text{Nb}_{0.012}\text{Se}_4)_2\text{I}$ at various frequencies.

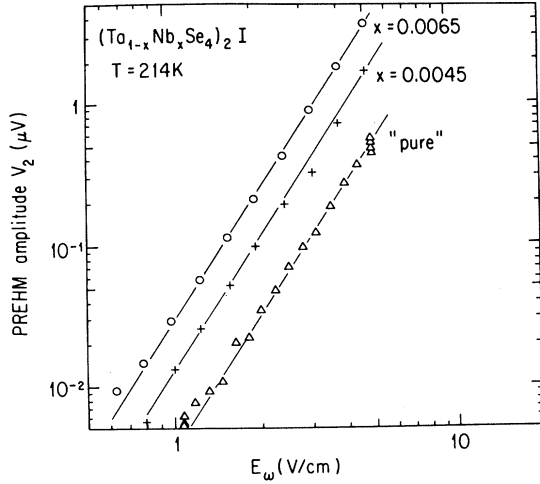


FIG. 7. Mixing-signal amplitude V_2 vs the amplitude E_ω of the fundamental frequency 9.5 GHz at a temperature of 214 K for nominally pure $(\text{TaSe}_4)_2\text{I}$ (Δ) and for $(\text{Ta}_{1-x}\text{Nb}_x\text{Se}_4)_2\text{I}$ with $x = 0.0045$ (+) and $x = 0.0065$ (\circ). The solid lines correspond to the relation $V_2 \sim E_\omega^3$.

III. ANALYSIS AND DISCUSSION

We first discuss the small-amplitude ac response observed, and compare findings with the various theoretical predictions. This is followed by the discussion of the nonlinear response.

A. Small-amplitude ac response

The experimental results presented above clearly show that a small amount of impurities has a profound effect on both the statics and dynamics of charge-density waves. The data displayed in Figs. 5 and 6 have been used to evaluate the frequency-dependent conductivity $\text{Re}\sigma(\omega)$ and $\text{Im}\sigma(\omega)$ at various temperatures, and the results are compared to the single harmonic-oscillator expression, Eq. (1). Typical results of both components of the conductivity obtained at three different temperatures are shown in Figs. 8, 9, and 10 for $(\text{Ta}_{1-x}\text{Nb}_x\text{Se}_4)_2\text{I}$. In both cases the solid lines are fits to

$$\text{Re}\sigma(\omega) = \frac{ne^2\tau^*}{m^*} \frac{(\omega/\tau^*)^2}{(\omega^2 - \omega_0^2)^2 + (\omega/\tau^*)^2}, \quad (3a)$$

$$\text{Im}\sigma(\omega) = \frac{ne^2\tau^*}{m^*} \frac{(\omega_0^2 - \omega^2)}{(\omega^2 - \omega_0^2)^2 + (\omega/\tau^*)^2}, \quad (3b)$$

where n is the density of electrons condensed in the CDW mode. Equations (3a) and (3b) follow from Eq. (1), and contributions to the finite spectral width from disorder-induced “inhomogeneous broadening”¹⁹ or possible band formation are neglected. For the response implied by Eq. (3), the dielectric constant is positive below ω_0 and negative above ω_0 and the conductivity $\text{Re}\sigma(\omega)$ reaches a maximum at ω_0 . Our experiments performed on $(\text{Ta}_{1-x}\text{Nb}_x\text{Se}_4)_2\text{I}$ alloys at several frequencies within each waveguide band clearly demonstrate that at high frequencies a description in terms of Eq. (3) is appropri-

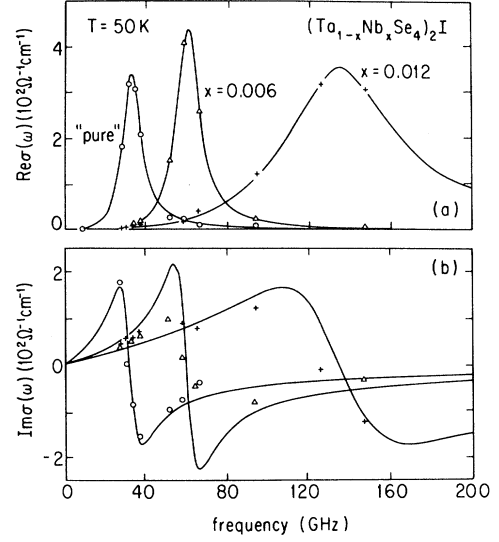


FIG. 8. Frequency dependence of $\text{Re}\sigma$ and $\text{Im}\sigma$ in $(\text{Ta}_{1-x}\text{Nb}_x\text{Se}_4)_2\text{I}$ alloys at 50 K. The solid lines are fits to Eq. (3) with parameters given in the text.

ate. In $(\text{TaSe}_4)_2\text{I}$, as in other materials,²³ a pronounced low-frequency tail is also observed.⁸ The effect reflects the internal deformations of the collective mode, and the dynamics of these deformations can be described both by a quantum-mechanical^{10,17} and classical^{11,18} approach. In our measured spectral range, low-frequency fluctuations are not important, and the frequency-dependent response is due to the oscillatory response of the collective mode, which is here described by an expression the same as that of a harmonic oscillator. Plots like those shown in Figs. 8, 9, and 10 were used to evaluate the parameters which characterize the pinned-mode resonance, m^* , τ^* , and ω_0 as a function of temperature and Nb con-

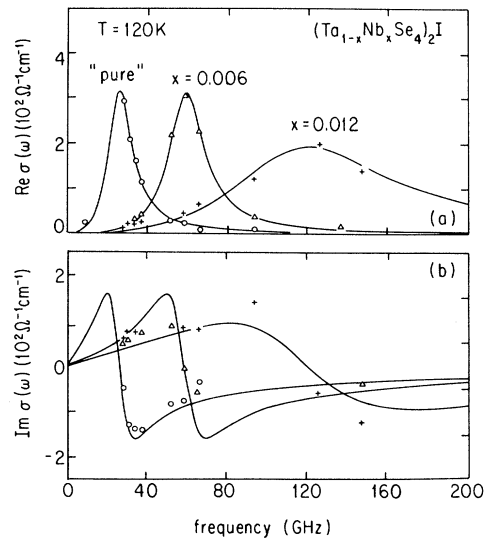


FIG. 9. Frequency dependence of $\text{Re}\sigma$ and $\text{Im}\sigma$ in $(\text{Ta}_{1-x}\text{Nb}_x\text{Se}_4)_2\text{I}$ alloys at 120 K. The solid lines are fits to Eq. (3) with parameters given in the text.

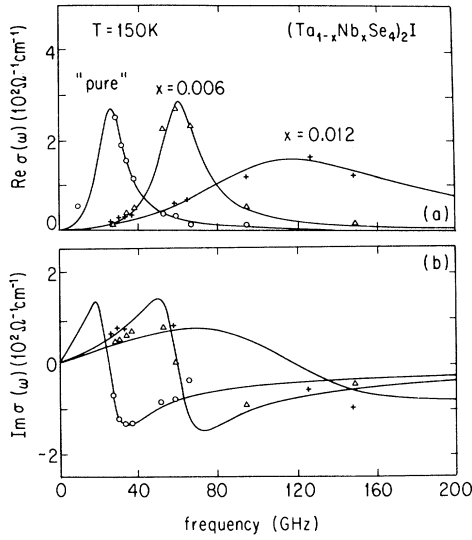


FIG. 10. Frequency dependence of $\text{Re}\sigma$ and $\text{Im}\sigma$ in $(\text{Ta}_{1-x}\text{Nb}_x\text{Se}_4)_2\text{I}$ alloys at 150 K. The solid lines are fits to Eq. (3) with parameters given in the text.

centration. Looking at Figs. 8–10, several qualitative features of our results are apparent. First, as noted earlier, there is a shift of spectral weight of the collective CDW response to higher frequencies with increasing impurity concentration. The frequency where the maximum conductivity occurs, $\omega_0/2\pi$, is increasing from approximately 28 GHz for the nominally pure samples to nearly 130 GHz for the samples with $x=0.012$, suggesting a strong increase of ω_0 with alloying, in agreement with the general concept of impurity pinning. Second, we observe a progressive broadening of the resonance with increasing impurity concentration, implying an impurity-induced relaxation mechanism which strongly contributes to the measured relaxation rate $\Gamma=1/(2\pi\tau^*)$. Third, the oscillator strength

$$\int \sigma_{\text{Re}}(\omega) d\omega = \frac{\pi}{2} \frac{ne^2}{m^*} \quad (4)$$

increases with increasing impurity concentration, suggesting a decreasing m^*/n value with increasing x .

The temperature dependence of ω_0 is displayed in Fig. 11 for the pure $(\text{TaSe}_4)_2\text{I}$ and for the alloys. In all cases only moderate temperature dependence is observed, and ω_0 slightly decreases with increasing temperature. This directly demonstrates that the pinning strength is independent of temperature in $(\text{TaSe}_4)_2\text{I}$. We believe that the concentration dependence of ω_0 found earlier for NbSe_3 and TaS_3 is not a fundamental behavior associated with charge-density-wave condensates, but is the consequence of partial gapping and commensurability effects.⁵ The concentration dependence of ω_0 is displayed in Fig. 12. Within our experimental error ω_0 increases linearly with the impurity concentration, clearly establishing experimentally that the collective mode is pinned by impurities in the alloys, with a residual impurity concentration or other lattice imperfections contributing to pinning in

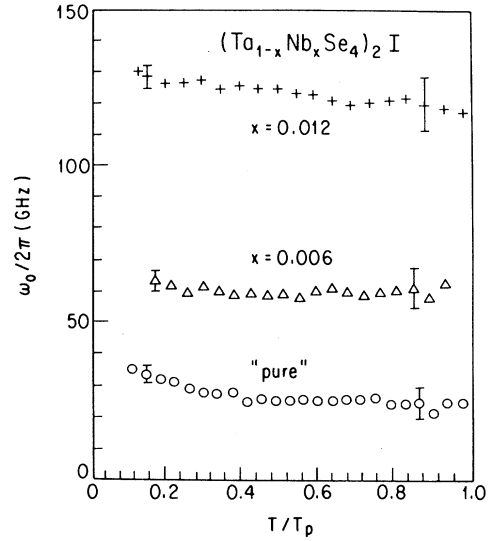


FIG. 11. Temperature dependence of $\omega_0/2\pi$ for $(\text{Ta}_{1-x}\text{Nb}_x\text{Se}_4)_2\text{I}$ alloys.

the nominally pure specimen.

The magnitude and temperature dependence of the effective mass is given, in terms of a mean-field theory^{24,25} by

$$\frac{m^*}{m}(T) = 1 + \lambda^{-1} \left[\frac{2\Delta(T)}{\omega_{2k_F}} \right]^2 f_0^{-1}(T), \quad (5)$$

where f_0 is the ratio of the number of condensed electrons to the total number of electrons, 2Δ the single-particle gap, λ the dimensionless electron-phonon coupling constant, and ω_{2k_F} the phonon frequency at wave vector $2k_F$ before the inclusion of the electron-phonon interactions. The temperature dependence of the effective masses is displayed in Fig. 13 with

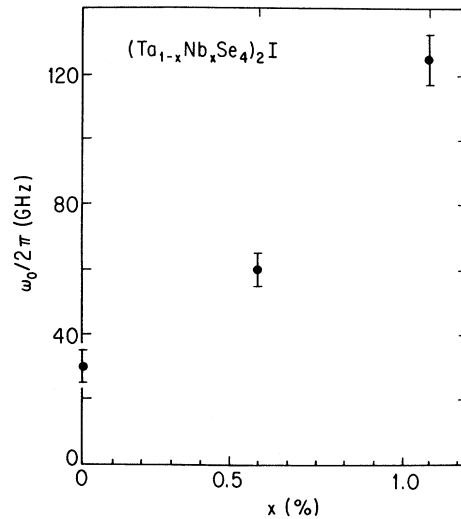


FIG. 12. Concentration dependence of $\omega_0/2\pi$ in $(\text{Ta}_{1-x}\text{Nb}_x\text{Se}_4)_2\text{I}$ alloys at low temperature.

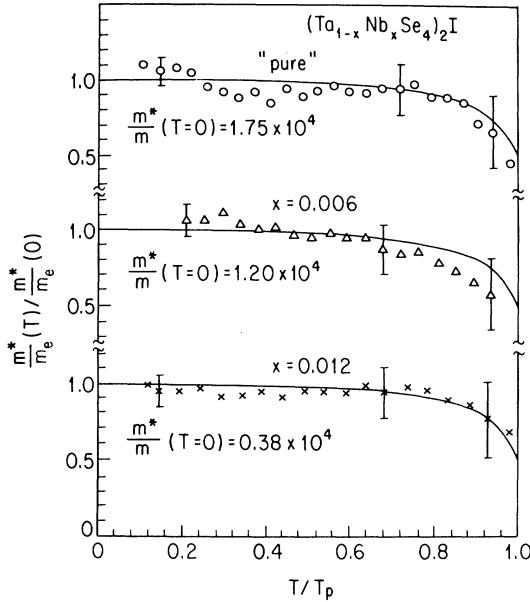


FIG. 13. Temperature dependence of m^*/m_e for $(\text{Ta}_{1-x}\text{Nb}_x\text{Se}_4)_2\text{I}$ alloys. The solid lines are the mean-field expression, Eq. (5).

$m^*/m(T=0)=1.75 \times 10^4$ for pure $(\text{TaSe}_4)_2\text{I}$, $m^*/m(T=0)=1.20 \times 10^4$ for 0.6% Nb: $(\text{TaSe}_4)_2\text{I}$, and $m^*/m(T=0)=0.38 \times 10^4$ for 1.2% Nb: $(\text{TaSe}_4)_2\text{I}$. The solid line in Fig. 13 is a theoretical curve $[m^*/m(T)]f_0^{-1}(T)$, reproducing well the overall behavior found experimentally. For pure $(\text{TaSe}_4)_2\text{I}$, m^*/m is also in good agreement with the mean-field expression (5), with the measured single-particle gap $\Delta \approx 1600$ K, estimated electron-phonon coupling constant²⁶ $\lambda \approx 0.6$, and phonon frequency $\omega_{2k_F} \approx 40$ K, these values giving $m^*/m(T=0) \approx 1.1 \times 10^4$.

The relation between the single-particle gap found from Fig. 2 and the effective mass is displayed in Fig. 14. The solid lines leads to

$$\frac{m^*}{m} = A \Delta^2, \quad (6)$$

with $A = 7.69 \times 10^{-3} \text{ K}^{-2}$, while from Eq. (5), with the previous values of λ and ω_{2k_F} we obtain a theoretical value $5.33 \times 10^{-3} \text{ K}^{-2}$. The agreement between theory and experiment is excellent, and we conclude, therefore, that mean-field theory, Eq. (5), describes well the magnitude, temperature, and concentration dependence of the effective mass in $(\text{TaSe}_4)_2\text{I}$ alloys. The magnitude of m^*/m was also found to be accounted for in other model compounds,¹ and we have shown earlier,²⁷ that $m^*(T)$ also follows the mean-field expression in $\text{K}_{0.3}\text{MoO}_3$.

The effect of impurities on the collective-mode response has been considered in detail by Fukuyama and Lee, and by Lee and Rice.¹⁹ Depending on the elastic constant associated with charge-density-wave deformations κ , the impurity concentration n_i , and potential V_0 , two limits can be distinguished.

For $\alpha = V_0 \rho_1 / 2 \kappa k_F n_i \gg 1$ (strong pinning), the

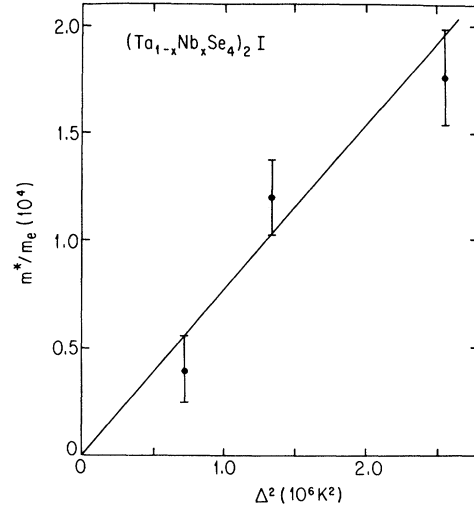


FIG. 14. $m^*/m_e(T=0)$ vs Δ^2 for $(\text{Ta}_{1-x}\text{Nb}_x\text{Se}_4)_2\text{I}$ alloys.

restoring-force constant k is given for three dimensions²⁸ by

$$k = \frac{4V_0 \rho_1 k_F^2}{\pi} n_i = A n_i \Delta = f_1(n_i), \quad (7a)$$

while for weak-impurity pinning

$$k = \frac{16k_F^5 V_0^2 \rho_1^2}{\pi \hbar^3 v_F^3} n_i^2 = B n_i^2 \Delta^4 = f_2(n_i), \quad (7b)$$

where A and B are constants.

The two parameters ω_0 and m^* can be combined to evaluate the concentration dependence of the total restoring force $k = m^* \omega_0^2$, and this parameter is displayed in Fig. 15. In Fig. 15 the solid line represents a restoring force which is proportional to the impurity concentration. We have also plotted in the figure the function $f_1 = n_i \Delta$ suggested by Eq. (7a) (dotted line), and it is evident that this also describes well our experimental findings. Both the solid and dotted lines imply a residual impurity concentration $n_{i,\text{res}} = 0.25\%$. In order to compare our findings with the weak-impurity-pinning model we used this value, and evaluated $f_2(n_i) = n_i^2 \Delta^4$ using the concentration dependence of the gap as given in Fig. 4. The dashed-dotted line is $f_2(n_i)$, normalized to the value obtained for $x = 1.2\%$. Although both the strong- and weak-pinning theories describe the main features of Fig. 15, a somewhat better agreement is obtained with the strong-pinning limit. Experiments on alloys with higher impurity concentrations would be required to distinguish clearly between weak- and strong-impurity pinning in $(\text{TaSe}_4)_2\text{I}$ alloys. The issue of whether weak- or strong-impurity pinning is occurring in various materials with a charge-density-wave ground state is highly controversial at present. Studies involving the pressure dependence of the threshold field²⁹ in $\text{K}_{0.3}\text{MoO}_3$ and impurity-doping studies³⁰ and NbSe_3 suggest weak pinning, while other studies also involving doping²¹ and irradiation³² are suggestive of strong pinning.

The temperature dependence of $1/\tau^*$ is displayed in

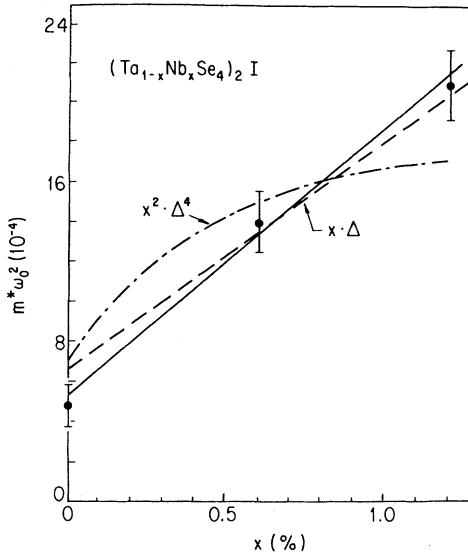


FIG. 15. Concentration dependence of $m^*\omega_0^2$ for $(\text{Ta}_{1-x}\text{Nb}_x\text{Se}_4)_2\text{I}$ alloys.

Fig. 16 for the pure compound and for the alloys. Two features are important: first, $1/\tau^*$ increases with increasing impurity concentration, and also $1/\tau^*$ in both pure $(\text{TaSe}_4)_2\text{I}$ and the alloys show a significant temperature dependence. This suggests that impurities play a significant role in the relaxation effects associated with the dynamics of the collective mode. This impurity-induced relaxation, however, does not lead to a temperature-independent additional relaxation, and (unlike as in the case for the Mathissen's rule) an empirical relation $1/\tau^* = 1/\tau_{\text{imp}}^* = 1/\tau^*(T)$ cannot describe our experimental findings. The enhancement of the relaxation time, however, appears to go hand in hand with the

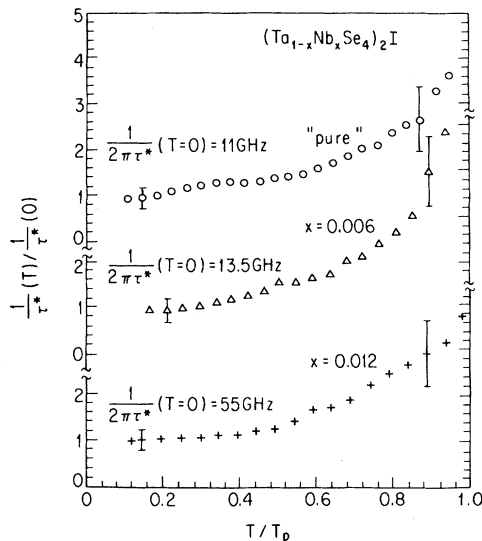


FIG. 16. Temperature dependence of $1/\tau^*$ for $(\text{Ta}_{1-x}\text{Nb}_x\text{Se}_4)_2\text{I}$ alloys.

effective mass, with the ratio τ^*/m^* independent of the impurity concentration. This feature is dominant in Fig. 17. The maximum conductivity of $\text{Re}\sigma(\omega)$ at frequency $\omega = \omega_0$ appears to follow a behavior that would be observed in the absence of a phase transition with metallic behavior. In the latter case $\sigma_{\text{dc}} = ne^2\tau/m$, where τ and m refer to the single-particle relaxation time and mass, while for the collective mode $\sigma(\omega = \omega_0) = ne^2\tau^*/m^*$. Consequently,

$$\frac{\tau^*}{m^*} \approx \frac{\tau}{m} \quad (8)$$

is approximately obeyed over a wide temperature range. Equation (8) has already been suggested by Bardeen,¹⁰ and has been shown to be valid near to the Peierls transition by Gor'kov and Dolgov.³³ This relation was found to be valid in other materials as well, such as TaS_3 and $\text{K}_{0.3}\text{MoO}_3$.¹

In Fig. 18 we give an overview of the overall temperature dependence of m^* , ω_0 , and $1/\tau^*$ for pure $(\text{TaSe}_4)_2\text{I}$ and for the alloys, in all cases the parameters being normalized to their $T=0$ value. For all of the fundamental parameters, the overall temperature dependence does not seem to be dependent on the impurity concentration, a result which—as has been discussed before—is understood for the pinning frequency ω_0 and effective mass m^* , but is unaccounted for as far as the relaxation rate $\Gamma = 1/\tau^*$ is considered.

B. Phase-resolved harmonic mixing

Two different models based on fundamentally different assumptions on the dynamics of the collective mode have been proposed earlier to describe the PREHM experiments in various model compounds. Both models^{17,18} lead to the same functional dependence of the mixing signal on the parameters which enter into the expressions which describe the small-amplitude ac response. Both models^{17,18} lead to a harmonic-mixing signal which is

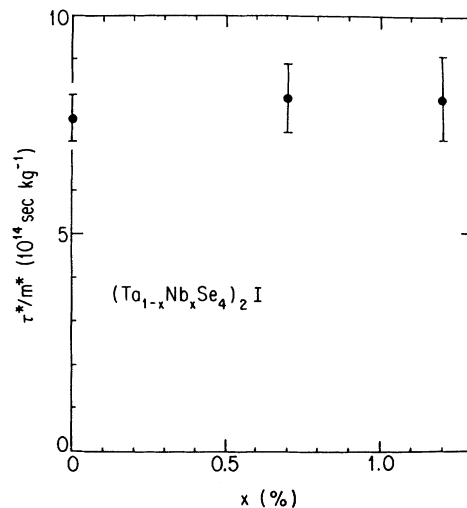


FIG. 17. Concentration dependence of τ^*/m^* at $T = 50 \text{ K}$ for $(\text{Ta}_{1-x}\text{Nb}_x\text{Se}_4)_2\text{I}$ alloys.

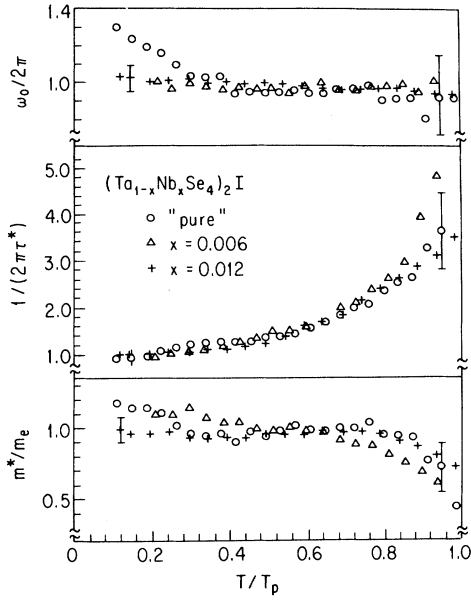


FIG. 18. Temperature dependence of $1/\tau^*$, m^*/m_e , and ω_0 . $1/\tau^*$ is normalized to the $T=0$ values for $(\text{Ta}_{1-x}\text{Nb}_x\text{Se}_4)_2\text{I}$ alloys.

given by $V_2 \sim E_\omega^3$, with E_ω the electric-field amplitude at the fundamental frequency ω . The results of the mixing experiments on pure $(\text{TaSe}_4)_2\text{I}$ have already been discussed elsewhere.¹⁶ It has been shown that the measured dependence of the mixing component V_2 on the microwave amplitude E_ω and on the fundamental frequency ω is in quantitative agreement with Bardeen's tunneling model¹⁷ which yields values for V_2 given by the dashed line in Fig. 7. The experimental results are also in semi-qualitative agreement with Matsukawa's calculation¹⁸ which is based on the Fukuyama-Lee-Rice (FLR) model. Here we focus on the concentration dependence of the parameters involved with the mixing-signal component V_2 reflecting the corresponding dependence of the Fröhlich mass m^* , of the pinning frequency ω_0 , and of the damping frequency $1/2\pi^*$ on impurities. The mixing signal, normalized to the $x=0$ value, is shown versus the Nb concentration in Fig. 19. In the tunneling model¹⁷ V_2 depends on ω_0 and on the threshold field E_T , and

$$V_2 \propto \omega_0^3 E_T^{-2}, \quad (9)$$

as already discussed in earlier papers.³⁴ Furthermore, the tunneling model yields the relation³⁵

$$E_T \propto \omega_0^2 m^*, \quad (10)$$

so that finally one obtains

$$V_2 \propto \omega_0^{-1} m^{*-2}. \quad (11)$$

The concentration dependence of V_2 can be calculated, using the concentration dependence of ω_0 and m^* as input parameters.

Matsukawa's calculation,¹⁸ which is based on a pertur-

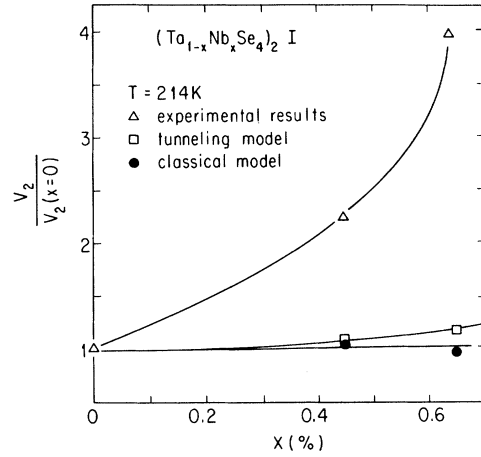


FIG. 19. Concentration dependence of the measured harmonic-mixing signal, together with the concentration dependence calculated from the classical and tunneling description of mixing.

bational analysis of the FLR model,¹⁹ results in a dependence of V_2 on the damping frequency instead of the dependence on ω_0 predicted by the tunnel model, and the appropriate relation is given by

$$V_2 \propto (2\pi\tau^*/m^*)^3, \quad (12)$$

and the concentration dependence expected can be inferred from the measured concentration dependence of τ^* and m^* .

In Fig. 19 we display the measured concentration dependence of the mixing signal together with the predictions of the tunneling and classical models, with the concentration dependence of the parameters ω_0 , m^*/m , and τ^* taken directly from the measured small-amplitude ac response (displayed in Figs. 12, 15, and 17). The data points referring to the "tunneling" and "classical" models are values of $\omega_0^{-1}m^{*-2}$ [see Eq. (11)] and τ^*/m^* [see Eq. (12)], normalized to these parameters obtained for the nominally pure material. As can be seen from the figure, both the classical and tunneling models predict a concentration dependence which is weaker than that obtained experimentally. The reason for this disagreement is not clear at present, it may reflect the slightly different current-voltage characteristics for the nominally pure compound and for the alloy. Qualitatively, the small-amplitude ac response may be—particularly at frequencies well below ω_0 —different from the simple form predicted by the various models. Indeed, recent experiments⁹ give a frequency-dependent conductivity $\sigma(\omega)$ which represents a contribution from both the oscillatory response of the rigid CDW and the response due to internal deformations. The dynamics of the latter has been described recently by defining a relaxation time τ , determined by momentum given to the electrons to relax to the charge-density waves. Earlier estimations¹⁰ give $\tau/\tau^* \simeq 60$ for the nominally pure compound; this ratio has, however, not been evaluated for the alloys. If the mixing experiments are determined by τ and τ^* in Eq. (12), an excellent agreement between theory and experi-

ment is obtained. Low-frequency conductivity measurements, together with harmonic-mixing experiments as the function of frequency, would be required to clarify this point.

IV. CONCLUSIONS

In this paper we reported a detailed study of the concentration dependent charge-density-wave dynamics in $(\text{Ta}_{1-x}\text{Nb}_x\text{Se}_4)_2\text{I}$ alloys. We find that the pinning frequency ω_0 increases with increasing x , demonstrating the importance of impurity pinning. The concentration dependence is suggestive for strong-impurity pinning; the pinning potential $m^*\omega_0^2$ increases linearly with increasing impurity concentration.

The effective mass decreases with increasing x , and this decrease goes hand in hand with the decrease of the single-particle gap Δ . Both the concentration and the temperature dependence of m^* can be described in terms of a mean-field description, a somewhat surprising result in light of the pronounced anisotropy of the material and the smearing of the transition by impurities. The relaxation rate is also concentration dependent, and moreover, the temperature dependence is also more pronounced to a higher impurity concentration. We also find that the concentration dependence at each temperature goes hand in hand with the concentration dependence of the effective mass, as suggested by various theories, but a microscopic theory is required to account for the magni-

tude, temperature, and concentration dependence of the relaxation effects.

Harmonic-mixing experiments are only in semiquantitative agreement with the various theories of charge-density-wave dynamics at microwave and millimeter-wave frequencies and mixing experiments conducted at different frequencies and temperatures are required to distinguish between the different models of the charge-density-wave dynamics. It is anticipated that the dynamics of the collective mode is different at radio and microwave frequencies, with the dynamics of the internal mode important in the low-frequency regime. This may explain the drastic difference between the conclusion based on experiments performed at different frequencies.

ACKNOWLEDGMENTS

The samples used in this study were prepared by M. Maki and B. Alavi. We also thank H. Fetterman for allowing us to use his equipment, which allowed experiments to be conducted at $f = 120$ GHz. Useful discussions with John Bardeen, K. Maki, K. Seeger, and A. Virosztek are gratefully acknowledged. This research was supported by NSF Grant No. DMR 89-13236 and by the United States of America–Austria Cooperative Science Program.

-
- ¹For a general review of the charge-density-wave dynamics, see G. Grüner, *Rev. Mod. Phys.* **60**, 1129 (1988), and references cited therein. *Charge-Density Waves in Solids*, edited by L. Gorkov and G. Grüner, Modern Problems in Condensed Matter Sciences, Vol. 25 (North-Holland, Amsterdam, 1989).
- ²Y. Imry and S.-k. Ma, *Phys. Rev. Lett.* **35**, 1399 (1975); L. J. Sham and B. R. Patton, *Phys. Rev. B* **13**, 3151 (1976).
- ³S. Sridhar, D. Reagor, and G. Grüner, *Phys. Rev. B* **24**, 2233 (1986).
- ⁴D. Reagor and G. Grüner, *Phys. Rev. Lett.* **56**, 659 (1986).
- ⁵D. Reagor and G. Grüner, *Phys. Rev. B* **39**, 7626 (1989).
- ⁶M. S. Sherwin, A. Zettl, and P. L. Richards, *Phys. Rev. B* **36**, 6708 (1987).
- ⁷H. P. Gesserich, G. Scheiber, M. Dorrlner, F. Lévy, and P. Monceau, *Physica B* **143**, 198 (1986).
- ⁸R. J. Cava, P. Littlewood, R. M. Fleming, R. G. Dunn, and E. A. Rietman, *Phys. Rev. B* **33**, 2439 (1986).
- ⁹S. Donovan *et al.*, *Solid State Commun.* **75**, 721 (1990); D. Reagor, S. Sridhar, M. Maki, and G. Grüner, *Phys. Rev. B* **32**, 8445 (1985).
- ¹⁰J. Bardeen, *Phys. Rev. Lett.* **62**, 2985 (1989); *Phys. Scr.* **T27**, 136 (1989).
- ¹¹T. Baier and W. Wonenberger, *Solid State Commun.* **72**, 773 (1989).
- ¹²J. R. Tucker, W. G. Lyons, and G. Gammie, *Phys. Rev. B* **38**, 1148 (1988).
- ¹³A. Philipp, W. Mayr, and K. Seeger, *Physica* **143B**, 27 (1986).
- ¹⁴A. Philipp, B. Hein, W. Mayr, and K. Seeger, *Solid State Commun.* **66**, 917 (1988).
- ¹⁵K. Seeger, A. Philipp, and W. Mayr, in *Proceedings of the 18th International Conference on the Physics of Semiconductors, Stockholm, 1986*, edited by O. Engstrom (World Scientific, Singapore, 1987), Vol. 2, pp. 1823–1826.
- ¹⁶A. Philipp, *Z. Phys. B* **75**, 31 (1989).
- ¹⁷J. Bardeen, *Phys. Rev. Lett.* **45**, 1978 (1980).
- ¹⁸H. Matsukawa, *J. Phys. Soc. Jpn.* **56**, 1522 (1987).
- ¹⁹H. Fukuyama, *J. Phys. Soc. Jpn.* **41**, 513 (1976); H. Fukuyama and P. A. Lee, *Phys. Rev. B* **17**, 535 (1978).
- ²⁰L. I. Buravov and I. F. Shchegolev, *Prib. Tekh. Eksp.* **171** (1971) [*Instrum. Exp. Tech.* **14**, 528 (1971)]; S. Sridhar, D. Reagor, and G. Grüner, *Rev. Sci. Instrum.* **56**, 1946 (1985); Tae Wan Kim, W. P. Beyermann, D. Reagor, and G. Grüner, *ibid.* **59**, 1219 (1988).
- ²¹W. Mayr, A. Philipp, and K. Seeger, *J. Phys. E* **19**, 135 (1986).
- ²²N. P. Ong, J. W. Brill, J. C. Eckert, J. W. Savage, S. K. Khanna, and R. B. Somoano, *Phys. Rev. Lett.* **42**, 811 (1979).
- ²³R. J. Cava, R. M. Fleming, R. G. Dunn, and E. A. Rietman, *Phys. Rev. B* **31**, 8325 (1985).
- ²⁴P. A. Lee, T. M. Rice, and P. W. Anderson, *Solid State Commun.* **14**, 703 (1974).
- ²⁵K. Maki and A. Virosztek, *Phys. Rev. B* **39**, 2511 (1989).
- ²⁶The expression $\Delta = 2\varepsilon_F \exp(-1/\lambda)$ gives with $\varepsilon_F = 0.4$ eV and $\Delta = 260$ K a value $\lambda = 0.6$.
- ²⁷Tae Wan Kim, D. Reagor, G. Grüner, K. Maki, and A. Virosztek, *Phys. Rev. B* **40**, 5372 (1989).
- ²⁸K. Maki and A. Virosztek, *Phys. Rev. B* **42**, 655 (1990).
- ²⁹G. Mihály and P. Canfield, *Phys. Rev. Lett.* **64**, 459 (1980).
- ³⁰N. P. Ong, J. W. Brill, J. C. Eckert, J. W. Savage, S. K. Khan-

- na, and R. B. Somoano, *Phys. Rev. Lett.* **42**, 811 (1979).
- ³¹M. Underweiser, M. Maki, B. Alavi, and G. Grüner, *Solid State Commun.* **64**, 181 (1987).
- ³²T. Chen and J. R. Tucker, *Phys. Rev. B* **41**, 7402 (1990); H. Mutka, S. Bouffard, G. Mihály, and L. Mihály, *J. Phys. (Paris) Lett.* **45**, L113 (1984); L. I. Schneemeyer, R. M. Fleming, and S. E. Spengler, *Solid State Commun.* **53**, 505 (1985).
- ³³L. P. Gor'kov and E. N. Dolgov, *Zh. Eksp. Teor. Fiz.* **77**, 396 (1979) [*Sov. Phys.—JETP* **50**, 203 (1979)].
- ³⁴K. Seeger, *Synth. Met.* **15**, 361 (1986).
- ³⁵J. Bardeen, *Z. Phys. B* **67**, 427 (1987).